

Merger states and final states of black hole coalescences: a numerical-relativity-assisted effective-one-body approach

Thibault Damour,¹ Alessandro Nagar,¹ and Loïc Villain²

¹*Institut des Hautes Études Scientifiques, 91440 Bures-sur-Yvette, France*

²*Laboratoire de Mathématiques et de Physique Théorique,*

Univ. F. Rabelais - CNRS (UMR 7350), Féd. Denis Poisson, 37200 Tours, France

(Dated: August 25, 2018)

We study to what extent the effective-one-body description of the dynamical state of a non-spinning, coalescing binary black hole (considered either at merger, or after ringdown) agrees with numerical relativity results. This comparison uses estimates of the integrated losses of energy and angular momentum during ringdown, inferred from recent numerical-relativity data. We find that the values, predicted by the effective-one-body formalism, of the energy and angular momentum of the system agree at the per mil level with their numerical-relativity counterparts, both at merger and in the final state. This gives a new confirmation of the ability of effective-one-body theory to accurately describe the dynamics of binary black holes even in the strong-gravitational-field regime. Our work also provides predictions (and analytical fits) for the final mass and the final spin of coalescing black holes for all mass ratios.

I. INTRODUCTION

The effective one body (EOB) formalism [1–6] has been introduced as a new analytical method for describing both the dynamics and the gravitational radiation of coalescing black-hole (BH) binaries during the entire coalescence process, from early inspiral to ringdown, passing through late inspiral, plunge and merger (see [7] for a recent EOB review). The EOB method started its development in 2000 (before the availability of numerical relativity (NR) simulations of coalescing BH's), and made several quantitative and qualitative predictions concerning the coalescence dynamics. These predictions have been broadly confirmed by subsequent NR simulations of merging BH's that started yielding reliable results after the NR breakthroughs of 2005 [8–10]. [See [11, 12] for reviews of NR results, and [13] for a recent impressive example of NR achievements]. As soon as NR simulations became available, a fruitful *synergy* between EOB and NR developed [14–18]. This synergy allowed one to complete the EOB formalism by incorporating some crucial *nonperturbative information* contained in NR results. This led to the definition of improved, NR-informed versions of the EOB formalism, sometimes referred to as EOBNR or EOB[NR] (see [19–24]).

Besides providing accurate gravitational waveforms (of direct interest for current gravitational wave detectors), the EOB formalism also gives a description of the *dynamics* of coalescing binaries. Several aspects of the EOB dynamical description have been (successfully) compared to NR results, notably: (i) gravitational recoil during coalescence [25], (ii) the spin parameter of the final BH [26], (iii) periastron advance during inspiral [27], and (iv) the functional relation between energy and angular momentum during inspiral [28]. The aims of the present work are, on the one hand, to update the early EOB-based study of the final spin of a (nonspinning) coalescing binary [26], and, on the other hand, to complete it

by considering the dynamical characteristics (energy and angular momentum) both of the *merger state* and of the *final state* of the BH system. [This aspect of our work is similar to the EOB/NR comparison done in [28].] On the EOB side our work will use the latest version of the (non-spinning, NR-informed) EOB formalism [24, 29], while, on the NR side, it will use the results of the most recent NR simulations of merging, unequal-mass BH binaries [30–35].

The paper is organized as follows: In Sec. II we compute from NR results the ringdown losses of energy and angular momentum. In Sec. III we compare the EOB prediction for the dynamical state of the BH system at merger to the corresponding state inferred from NR results, while Sec. IV performs such an EOB/NR comparison for the final dynamical state. Some conclusions are presented in Sec. V. We use geometric units $G = c = 1$. The letter q is used to denote the mass ratio $q := m_2/m_1 \geq 1$, while ν denotes the symmetric mass ratio $\nu := m_1 m_2 / (m_1 + m_2)^2 = q / (q + 1)^2$.

II. NR-COMPUTED RINGDOWN LOSSES OF ENERGY AND ANGULAR MOMENTUM

Throughout this paper we shall (conventionally) call “merger” the moment t^{mrg} when the modulus of the $lm = 22$ strain waveform $h_{22}(t)$ [or, equivalently, its Zerilli-normalized version $\Psi_{22}(t) = (R/M)h_{22}/\sqrt{24}$] reaches its maximum. We correspondingly refer to the phase following the merger, i.e. $t > t^{\text{mrg}}$, as being the “ringdown”. We shall apply these definitions both to the NR waveform, and to the EOB one. In other words, the NR merger moment $t_{\text{NR}}^{\text{mrg}}$ is computed by considering the maximum of the modulus of the NR waveform as a function of the NR time scale, while the EOB merger moment $t_{\text{EOB}}^{\text{mrg}}$ is computed from the maximum of the EOB waveform as a function of the EOB time scale. In the present

Section we only consider the NR waveform, and shall estimate the (NR) losses (in the form of fluxes at infinity) of energy and angular momentum during the NR ringdown, $t_{\text{NR}} > t_{\text{NR}}^{\text{mrg}}$. [For brevity, we suppress in the formulas of this Section the label NR on all the quantities.]

Using the Zerilli-normalization of the waveform $\Psi_{\ell m}(t) = (R/M)h_{\ell m}/\sqrt{(\ell+2)(\ell+1)\ell(\ell-1)}$ the fluxes of energy and angular momentum at infinity are given by

$$\dot{E}_{(\ell_{\text{max}})} = \frac{1}{16\pi} \sum_{\ell=2}^{\ell_{\text{max}}} \sum_{m=-\ell}^{\ell} \frac{(\ell+2)!}{(\ell-2)!} |\dot{\Psi}_{\ell m}|^2, \quad (1)$$

$$\dot{J}_{(\ell_{\text{max}})} = -\frac{1}{8\pi} \sum_{\ell=2}^{\ell_{\text{max}}} \sum_{m=1}^{\ell} m \frac{(\ell+2)!}{(\ell-2)!} \Im \left[\dot{\Psi}_{\ell m} \Psi_{\ell m}^* \right], \quad (2)$$

where the summation over ℓ extends only up to some maximum value ℓ_{max} and $\Psi_{\ell m}^* = (-1)^m \Psi_{\ell, -m}$. The corresponding (NR) ringdown losses are then obtained by integrating the fluxes (1), (2) over $t > t^{\text{mrg}}$, namely

$$E_{(\ell_{\text{max}})}^{\text{rgd}} = \int_{\text{merger}}^{\infty} dt \dot{E}_{(\ell_{\text{max}})} = \sum_{\ell=2}^{\ell_{\text{max}}} E_{\ell}^{\text{rgd}}, \quad (3)$$

$$J_{(\ell_{\text{max}})}^{\text{rgd}} = \int_{\text{merger}}^{\infty} dt \dot{J}_{(\ell_{\text{max}})} = \sum_{\ell=2}^{\ell_{\text{max}}} J_{\ell}^{\text{rgd}}. \quad (4)$$

Here the last expressions on the right denote the decomposition of the integrated ringdown losses into individual multipolar contributions, obtained by fixing ℓ and summing over m in Eqs. (1), (2). [Note the notational difference between, say, the individual contribution E_{ℓ}^{rgd} and the result of its summation up to ℓ_{max} : $E_{(\ell_{\text{max}})}^{\text{rgd}}$.]

The NR waveform data available to us have been computed with the SpEC code by the Caltech-Cornell-CITA collaboration [30, 31]. For the mass ratio $q = m_2/m_1 = 1$ [30], all waveform multipoles up to $\ell_{\text{max}} = 8$ are present. When $q \geq 2$ [31], only the dominant ℓm multipoles up to $\ell_{\text{max}} = 6$ are available, namely $\ell m = (22, 21, 33, 31, 44, 55, 66)$. Starting from this information we tried to improve the determination of the ringdown losses $E_{(\ell_{\text{max}})}^{\text{rgd}}, J_{(\ell_{\text{max}})}^{\text{rgd}}$ by studying the decay of the partial multipolar contributions $E_{\ell}^{\text{rgd}}, J_{\ell}^{\text{rgd}}$ entering the above sums as ℓ increases. When $q \leq 2$ we found that the decay, as ℓ increases, of $E_{\ell}^{\text{rgd}}, J_{\ell}^{\text{rgd}}$ is *non monotonic*. More precisely, we found that, when $q \leq 2$, the partial multipolar contributions $E_{\ell}^{\text{rgd}}, J_{\ell}^{\text{rgd}}$ corresponding to even or odd values of ℓ behave in different ways. However, if we compare the even and odd contributions among themselves, they seem to form two independent geometric sequences as functions of ℓ . In other words, for sufficient large values of ℓ , we have (when grouping together either even or odd values of ℓ) $\ln E_{\ell}^{\text{rgd}} \propto -\ell$, $\ln J_{\ell}^{\text{rgd}} \propto -\ell$. This behavior is illustrated in Fig. 1 for

the $q = 1$ and $q = 2$ cases. Note that such a simple decay law $\propto \exp(-c\ell)$ is suggested by the leading-order post-Newtonian (PN) expression of the various multipoles, namely $h_{\ell m} \propto n_{\ell m}^{(\epsilon)} c_{\ell+\epsilon}(\nu) v_{\varphi}^{\ell+\epsilon} \exp(-im\Phi)$, where $\epsilon = 0, 1$ denotes the parity, $n_{\ell m}^{(\epsilon)}$ is a parity-dependent numerical factor, $c_{\ell+\epsilon}(\nu)$ a mass-ratio dependent one, $v_{\varphi} = r_{\omega} \Omega$ a suitably defined (and resummed) azimuthal velocity, and Φ the orbital phase; see [6]. Previous EOB studies have shown that such ‘‘Newtonian-order’’ expressions (after a suitable resummation of the PN corrections) stay numerically close to the full NR waveform essentially up to merger. As the value of v_{φ} at merger is still smaller than one (and as the orbital motion stays quasi-circular till merger), we can indeed expect a simple parity-dependent ℓ -exponential decay of the multipolar contributions to the fluxes $\dot{E}_{\ell}, \dot{J}_{\ell}$. [Actually, the ℓ behavior of the fluxes results from combining various ℓ -dependent factors; in addition, one must take into account the effect of time-integration. Anyway, our phenomenological findings are useful independently of any precise analytical justification.]

This leads us to introduce separate, even or odd, decay ratios, say (using the fact that, in the case at hand, ℓ_{max} is even)

$$r_e^E = E_{\ell_{\text{max}}}^{\text{rgd}} / E_{\ell_{\text{max}}-2}^{\text{rgd}}, \quad (5)$$

$$r_o^E = E_{\ell_{\text{max}}-1}^{\text{rgd}} / E_{\ell_{\text{max}}-3}^{\text{rgd}}, \quad (6)$$

$$r_e^J = J_{\ell_{\text{max}}}^{\text{rgd}} / J_{\ell_{\text{max}}-2}^{\text{rgd}}, \quad (7)$$

$$r_o^J = J_{\ell_{\text{max}}-1}^{\text{rgd}} / J_{\ell_{\text{max}}-3}^{\text{rgd}}. \quad (8)$$

Here, we used as best estimates of the E and J decay ratios the largest- ℓ 's we can consider. As we shall see later, the numerical values of the E and J decay ratios are found to be approximately equal: $r_e^E \approx r_e^J \approx r_o^E \approx r_o^J$, but we did not use this approximate fact in our analysis.

In view of this simple geometric-series decay of the multipolar contributions to the ringdown losses, we can improve their ℓ_{max} -truncated estimates (3), (4) by summing the two separate geometric series representing the higher- ℓ contributions. This leads to the following ‘‘corrected’’ estimate of the NR ringdown losses (still in the case $q \leq 2$)

$$\begin{aligned} E_{\text{corr.}}^{\text{rgd}} &= \sum_{\ell=2}^{\infty} E_{\ell}^{\text{rgd}} \\ &= E_{(\ell_{\text{max}})}^{\text{rgd}} + E_{\ell_{\text{max}}}^{\text{rgd}} \frac{r_e^E}{1-r_e^E} + E_{\ell_{\text{max}}-1}^{\text{rgd}} \frac{r_o^E}{1-r_o^E}, \end{aligned} \quad (9)$$

$$\begin{aligned} J_{\text{corr.}}^{\text{rgd}} &= \sum_{\ell=2}^{\infty} J_{\ell}^{\text{rgd}} \\ &= J_{(\ell_{\text{max}})}^{\text{rgd}} + J_{\ell_{\text{max}}}^{\text{rgd}} \frac{r_e^J}{1-r_e^J} + J_{\ell_{\text{max}}-1}^{\text{rgd}} \frac{r_o^J}{1-r_o^J}. \end{aligned} \quad (10)$$

The values of the ratios $r_{e,o}^{E,J}(q)$ we obtained are: (i) for $q = 1$; $r_e^E = 0.02908, r_o^E = 0.03272, r_e^J = 0.02857, r_o^J =$

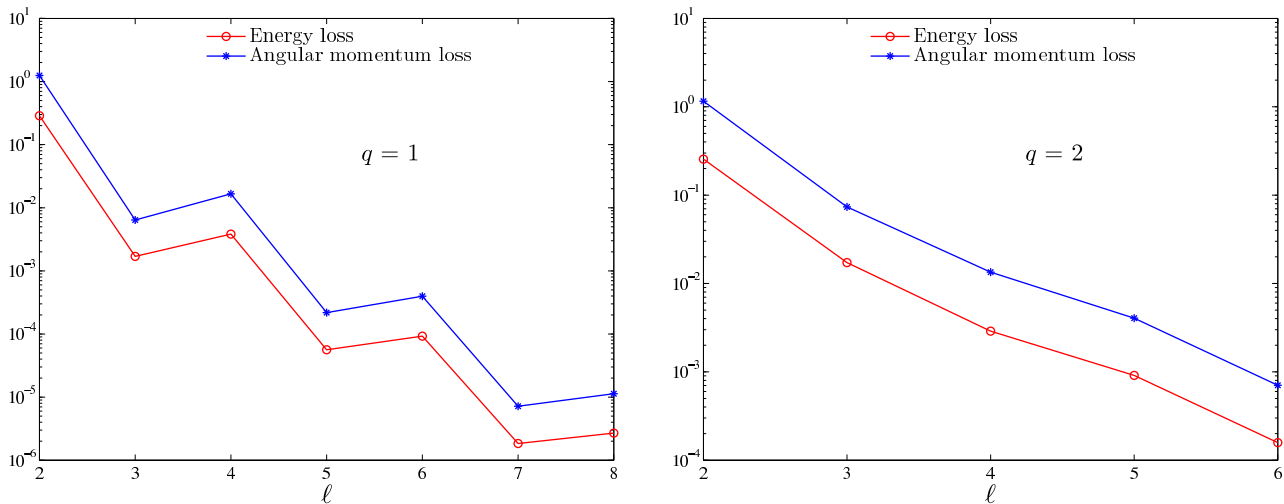


FIG. 1. Logarithms of the ℓ -th multipolar contributions, E_ℓ^{rgd} , J_ℓ^{rgd} , to the ringdown losses, as functions of ℓ for $q = 1$ (left) and $q = 2$ (right), exhibiting different behaviors for even and odd values of ℓ ; the difference becomes less pronounced as q increases.

0.03286 and (ii) for $q = 2$; $r_e^E = 0.05467$, $r_o^E = 0.05280$, $r_e^J = 0.05249$, $r_o^J = 0.05495$.

from the highest possible value of ℓ ,

$$r^E = E_{\ell_{\text{max}}}^{\text{rgd}} / E_{\ell_{\text{max}}-1}^{\text{rgd}}, \quad (11)$$

$$r^J = J_{\ell_{\text{max}}}^{\text{rgd}} / J_{\ell_{\text{max}}-1}^{\text{rgd}}. \quad (12)$$

This common ratio would be related to the separate ones introduced above via $r_o = r_e = r^2$. The corresponding improved estimate of the total ringdown losses is then obtained as

$$E_{\text{corr}}^{\text{rgd}} = \sum_{\ell=2}^{\infty} E_\ell^{\text{rgd}} = E_{(\ell_{\text{max}})}^{\text{rgd}} + E_{\ell_{\text{max}}}^{\text{rgd}} \frac{r^E}{1 - r^E}, \quad (13)$$

$$J_{\text{corr}}^{\text{rgd}} = \sum_{\ell=2}^{\infty} J_\ell^{\text{rgd}} = J_{(\ell_{\text{max}})}^{\text{rgd}} + J_{\ell_{\text{max}}}^{\text{rgd}} \frac{r^J}{1 - r^J}. \quad (14)$$

The values of the ratios $r^{E,J}(q)$ we obtained for $q \geq 3$ are: (i) for $q = 3$; $r^E = 0.2918$, $r^J = 0.2871$, (ii) for $q = 4$; $r^E = 0.3339$, $r^J = 0.3315$, and (iii) for $q = 6$; $r^E = 0.3730$, $r^J = 0.3795$.

The final results we obtained by this method are displayed in Table I. Let us recall that these results are based: for $q = 1$ on the results of [30], and for $q = 2, 3, 4, 6$ on the results of [31]. For the case $q = 1$ we had data up to $\ell_{\text{max}} = 8$ while for the other NR data we had data only up to $\ell_{\text{max}} = 6$. In addition, we report in this Table the corresponding results for the test-mass case $q = \infty$ (actually $q = 10^3$), based on the results of [35]. For that case, we had data up to $\ell_{\text{max}} = 8$. In the table we indicate both the “uncorrected” values of the losses (up to ℓ_{max} or $\ell_{\text{max}} - 2$), and the corrected ones.

The ringdown losses displayed in Table I have been scaled by a factor ν^2 because each multipolar waveform $\Psi_{\ell m}(t) = (R/M)h_{\ell m} / \sqrt{(\ell+2)(\ell+1)\ell(\ell-1)}$ contains a factor ν which is conveniently factored out. In our previous work [26], we had proposed to approximate the ν dependence of the ringdown losses by assuming that this

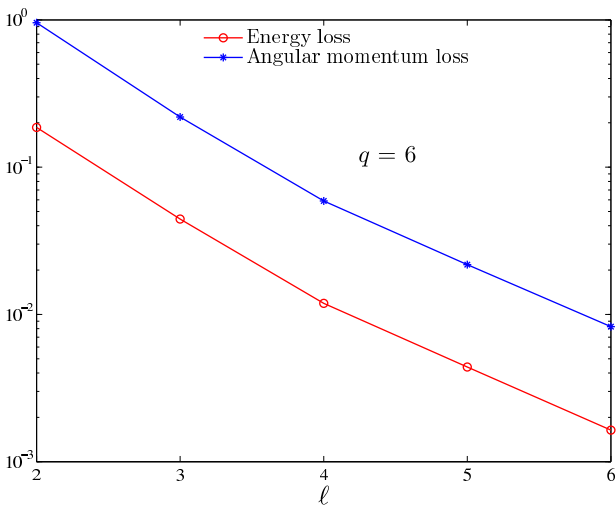


FIG. 2. Logarithms of the ℓ -th multipolar contributions, E_ℓ^{rgd} , J_ℓ^{rgd} , to the ringdown losses, as functions of ℓ for $q = 6$, exhibiting a uniform behavior for even and odd values of ℓ .

Fig. 1 showed that the pronounced even/odd difference present when $q = 1$ is already much weaker when $q = 2$. For larger values of q , namely $q \geq 3$, we found a uniform ℓ -behavior in that the even and odd partial contributions arrange themselves (for large enough ℓ) along a *common* geometric-series. See, as an illustration, Fig. 2 for the $q = 6$ case. In other words, there is no need to introduce separate even and odd ratios, and one can simply introduce a common ratio between $\ell - 1$ and ℓ , say estimated

TABLE I. NR losses of energy and angular momentum during ringdown, i.e. after the maximum of h_{22}^{NR} .

ν	q	ℓ_{max}	E^{rgd}/ν^2	J^{rgd}/ν^2	$E_{\text{corr.}}^{\text{rgd}}/\nu^2$	$J_{\text{corr.}}^{\text{rgd}}/\nu^2$
0	∞	8	0.267836	1.51821	0.270011	1.53037
0	∞	6	0.262383	1.48763		
0.1224...	6	6	0.248517	1.26535	0.249492	1.27041
0.16	4	6	0.254961	1.24448	0.255392	1.24651
0.1875	3	6	0.263139	1.24301	0.263344	1.24393
$0.\bar{2}$	2	6	0.276747	1.24870	0.276807	1.24898
0.25	1	6	0.293199	1.27188		
0.25	1	8	0.293204	1.27190	0.293204	1.27190

ν^2 scaling holds for any value of ν . This would correspond to assuming that the ratios $E_{\text{corr.}}^{\text{rgd}}/\nu^2$, $J_{\text{corr.}}^{\text{rgd}}/\nu^2$ do not depend on ν . As we see on Table I, this assumption is approximately correct. For instance, as ν varies between 0 (test-mass case) and 1/4 (equal-mass case), $E_{\text{corr.}}^{\text{rgd}}/\nu^2$ varies between 0.27 and 0.29, passing through a minimum $\simeq 0.25$. Similarly, $J_{\text{corr.}}^{\text{rgd}}/\nu^2$ varies between 1.53 and 1.27, passing through a minimum $\simeq 1.24$. Compared to the ν^2 scaling, these are rather mild variations. Let us also note that the effect of higher multipoles is fractionally more important as ν becomes small. This explains why our current best estimates of the corrected values of $E_{\text{corr.}}^{\text{rgd}}/\nu^2$, $J_{\text{corr.}}^{\text{rgd}}/\nu^2$ for $\nu \rightarrow 0$, namely 0.27001 and 1.53037 significantly differ from the corresponding values, 0.2448 and 1.3890 we had used in [26], which were based on summing only up to $\ell_{\text{max}} = 4$ multipoles.

Before discussing in more detail the relative importance of the various multipolar orders to the results in Table I, let us mention that the final, corrected values listed there (for a sample of q values) can be approximately represented by the following polynomials in ν :

$$\begin{aligned} E_{\text{corr.}}^{\text{rgd}}/\nu^2 &= 2.0337\nu^2 - 0.41783\nu + 0.27005, \\ J_{\text{corr.}}^{\text{rgd}}/\nu^2 &= 8.3205\nu^2 - 3.1076\nu + 1.5298. \end{aligned} \quad (15)$$

These ν -dependent fits reproduce the values of the *unscaled* ringdown losses $E_{\text{corr.}}^{\text{rgd}}$, $J_{\text{corr.}}^{\text{rgd}}$ corresponding to the above-listed q -sample of scaled losses modulo differences smaller than -4.1×10^{-5} for $E_{\text{corr.}}^{\text{rgd}}$ (fit minus exact difference reached when $q = 2$), and $+1.5 \times 10^{-4}$ for $J_{\text{corr.}}^{\text{rgd}}$ (fit minus exact difference reached when $q = 3$). In the following, we shall use these fits only when we will need an estimate of the ringdown losses in the range $0 < \nu < 0.1224$ where we do not have sufficient NR data to estimate them by the method explained above.

As it can happen that one does not have at hand NR data covering higher multipolar contributions, it is useful to study which fraction of the total ringdown losses is due to the dominant $\ell m = 22$ (even) quadrupolar waveform, and which fraction is due to the subdominant contributions (i.e., in the present context, the subdominant quadrupolar waveforms $\ell m = 21$ and $\ell m = 20$, as well

as the higher multipolar orders $\ell \geq 3$). Let us define the fractional contribution of subdominant multipoles to the ringdown losses as

$$f_E = \frac{E_{\text{corr.}}^{\text{rgd}} - E_{22}^{\text{rgd}}}{E_{\text{corr.}}^{\text{rgd}}}, \quad (16)$$

$$f_J = \frac{J_{\text{corr.}}^{\text{rgd}} - J_{22}^{\text{rgd}}}{J_{\text{corr.}}^{\text{rgd}}}, \quad (17)$$

so that, e.g., $E_{\text{corr.}}^{\text{rgd}} = E_{22}^{\text{rgd}}/(1 - f_E)$, etc.

We give in Table II the values of the fractions f_E and f_J for the q values we studied here. The ν dependence of f_E and f_J is illustrated in Fig. 3. This figure plots both the points listed in Table II, and the following polynomial fits to f_E and f_J

$$f_E = -1.51473\nu^2 - 1.54739\nu + 0.502328, \quad (18)$$

$$f_J = -1.32120\nu^2 - 1.45965\nu + 0.467261. \quad (19)$$

TABLE II. Relative contribution of all subdominant terms (i.e. different from $\ell = m = 2$) to the total ringdown losses of energy and angular momentum: $f_Q = 1 - Q_{22}^{\text{rgd}}/Q_{\text{corr.}}^{\text{rgd}}$ with $Q = E$ or J .

ν	q	f_E	f_J
0	∞	0.502552	0.467411
0.1224...	6	0.287962	0.267059
0.16	4	0.216489	0.200202
0.1875	3	0.160672	0.148506
$0.\bar{2}$	2	0.0846702	0.0785165
0.25	1	0.0193487	0.0185868

Table II and Fig. 3 show that the fractions f_E and f_J *strongly depend* on ν . More precisely, while the $\ell = m = 2$ waveform contributes alone most of the ringdown losses when one is close to the equal-mass case $\nu \simeq 0.25$, it contributes only about half of the total losses when one

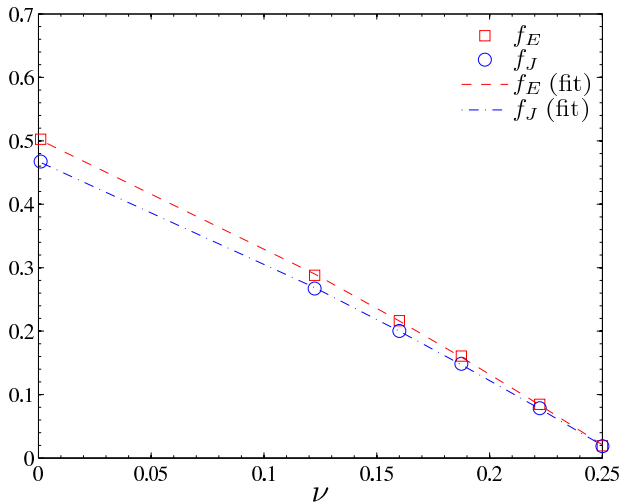


FIG. 3. Fraction of the total ringdown losses of energy and angular momentum (resp. f_E and f_J) due to higher multipoles ($\ell m \neq 22$) as functions of ν for NR data and the test-mass values. Both corrected values and the fits Eqs. (18) and (19) are plotted.

is close to the extreme-mass ratio case $\nu \ll 1$. However, we hope that our fits (18), (19) can provide a useful alternative to using many NR multipoles, by simply dividing the $\ell m = 22$ NR ringdown contributions by the corresponding factors $1 - f_E(\nu)$ or $1 - f_J(\nu)$.

III. DYNAMICAL STATE AT MERGER: NR/EOB COMPARISON

In this Section we shall compare the analytical EOB prediction for the dynamical state of the system at merger to the corresponding result that can be inferred from NR data. Here, like in any EOB work, the word “analytical” is to be understood in the sense that the EOB formalism provides a set of analytical equations of motion for the dynamical state of the system. These equations are, however, too complex to be solved exactly, and one resorts to standard (Runge-Kutta-type) numerical tools to obtain their solutions. Due to the sensitivity to the EOB initial conditions, in most cases the EOB results given below with six significant digits are actually accurate within fractional errors of order 10^{-5} .

From the NR side, if we start from the *final* values of the energy and angular momentum of the system (i.e. the mass M_f and angular momentum J_f of the final BH resulting from the coalescence of the two BH’s), we can estimate the energy and angular momentum of the system at the moment of merger, say $E_{\text{NR}}^{\text{mrg}}$, and $J_{\text{NR}}^{\text{mrg}}$, by adding to M_f and J_f the corresponding ringdown losses:

$$E_{\text{NR}}^{\text{mrg}} := M_f^{\text{NR}} + E_{\text{NR}}^{\text{rgd}}, \quad (20)$$

$$J_{\text{NR}}^{\text{mrg}} := J_f^{\text{NR}} + J_{\text{NR}}^{\text{rgd}}. \quad (21)$$

Here, for clarity, we added a subscript NR to the (cor-

rected) NR ringdown losses estimated in the previous Section. We added also a superscript NR to M_f and J_f . Indeed, we took for them the values directly indicated in the original NR papers [30, 31], without using the various approximate fitting formulas for them that have been proposed in the literature [22, 26, 36–39].

From the EOB side, the EOB code computes at any moment (on the EOB time axis) the total energy $E_{\text{EOB}}(t) = H(t)$ and total angular momentum $J_{\text{EOB}}(t) = \nu p_\varphi(t)$ of the binary system. To compute the values of $E_{\text{EOB}}(t)$ and $J_{\text{EOB}}(t)$ at (EOB) merger we just need to know (from the EOB code itself) what moment $t_{\text{EOB}}^{\text{mrg}}$ on the EOB time axis corresponds to “merger”. The (conventional) definition we gave above of “merger” is equally meaningful within the NR context and within the EOB one. In other words, the EOB merger moment is simply the (EOB) time $t_{\text{EOB}}^{\text{mrg}}$ when the modulus of the $\ell m = 22$ EOB strain waveform $h_{22}^{\text{EOB}}(t)$ reaches its maximum. The (EOB) merger energy and angular momentum are then:

$$E_{\text{EOB}}^{\text{mrg}} := E_{\text{EOB}}(t_{\text{EOB}}^{\text{mrg}}), \quad (22)$$

$$J_{\text{EOB}}^{\text{mrg}} := J_{\text{EOB}}(t_{\text{EOB}}^{\text{mrg}}). \quad (23)$$

Here, we have been using the fact that, within the EOB formalism, there is well-defined link between the dynamical time, and the (retarded) time used to express the waveform. The EOB waveform used here to find $t_{\text{EOB}}^{\text{mrg}}$ is the inspiral-plus-plunge waveform defined in Eq. (16) of [24], including the next-to-quasi-circular correction factor $\hat{h}_{\ell m}^{\text{NQC}}$ of Eq. (27) there. As the maximum of $|h_{22}|$ occurs *before* the (EOB) moment $t_{\Omega \text{ peak}}^{\text{EOB}}$ where the orbital frequency Ω peaks (and where one attaches the sum of quasi-normal modes modelling the ringdown), the determination of EOB merger does not depend on this quasi-normal-mode attachment procedure. On the other hand, the determination of EOB merger is not a purely analytical procedure that directly follows from analytically known first principles. It is a procedure that depends both on the analytically known part of EOB, and on the NR-informed improvements leading to the current EOB[NR] formalism. Notably, the determination of the precise value of $t_{\text{EOB}}^{\text{mrg}}$ involves the knowledge of the parameters a_i entering the modulus of the next-to-quasi-circular correction factor $\hat{h}_{22}^{\text{NQC}}$ to the $\ell m = 22$ waveform. These parameters have been determined in [24] (as functions of ν) by extracting some non-perturbative information from NR waveforms (namely the shape of the NR modulus $|h_{22}^{\text{NR}}(t^{\text{NR}})|$ near a certain NR instant $t_{\text{extr}}^{\text{NR}}$, located just after $t_{\text{NR}}^{\text{mrg}}$).

The comparison between the pure NR quantities $E_{\text{NR}}^{\text{mrg}}$, $J_{\text{NR}}^{\text{mrg}}$ and the corresponding EOB[NR] ones $E_{\text{EOB}}^{\text{mrg}}$, $J_{\text{EOB}}^{\text{mrg}}$ is presented in Table III. The NR/EOB agreement is quite good, both for E^{mrg} and for J^{mrg} . It is essentially at the 10^{-3} (fractional) level, which is remarkable when one thinks that the physically complicated merging two-black-hole system we are considering is represented (at the time $t_{\text{EOB}}^{\text{mrg}} < t_{\Omega \text{ peak}}^{\text{EOB}}$), in the EOB formalism, by means of a rather simple analytic Hamiltonian (corresponding to a two point-mass system). To put this level

TABLE III. Total energy and angular momentum at the time of merger for NR and EOB (see the text).

ν	q	$E_{\text{NR}}^{\text{mrg}}$	$E_{\text{EOB}}^{\text{mrg}}$	$J_{\text{NR}}^{\text{mrg}}$	$J_{\text{EOB}}^{\text{mrg}}$
0.1224...	6	0.98921(5)	0.989495	0.38075(10)	0.380534
0.16	4	0.98446(2)	0.984978	0.48292(10)	0.482790
0.1875	3	0.98054(1)	0.981218	0.55371(2)	0.553486
0.2	2	0.97491(2)	0.975784	0.63773(4)	0.637243
0.25	1	0.96995(2)	0.971156	0.70114(4)	0.702198

of NR/EOB agreement in perspective let us note that the purely NR check of the conservation of energy and angular momentum (between the initial state and the final state of a $q = 1$ system) done in [40] yielded fractional agreements of order $|E_{\text{NR}}^{\text{in}} - E_{\text{NR}}^{\text{rad}} - E_{\text{NR}}^{\text{f}}|/E_{\text{NR}}^{\text{f}} = 7.6 \times 10^{-5}$ and $|J_{\text{NR}}^{\text{in}} - J_{\text{NR}}^{\text{rad}} - J_{\text{NR}}^{\text{f}}|/J_{\text{NR}}^{\text{f}} = 5.5 \times 10^{-4}$.

Let us also note that the EOB merger energies are systematically *larger* than the NR ones. This (small) systematic difference might simply be due to the fact (already emphasized in [28]) that, in using the consequences of simple conservation laws for E and J , we have neglected the ‘‘Schott contributions’’ to E and J . This issue has been recently studied within the EOB formalism [41]. The latter reference showed that (with the choice of radiation reaction adopted in the present EOB formalism [24]), only the energy had a Schott contribution $E_{\text{EOB}}^{\text{Schott}}$, and that this contribution was small during the inspiral and was *negative* (because proportional to the radial momentum). This result actually means that, when defining the NR merger energy as above, it should be compared to the sum $E_{\text{EOB}}^{\text{mrg}} + E_{\text{EOB}}^{\text{Schott}} < E_{\text{EOB}}^{\text{mrg}}$, rather than to $E_{\text{EOB}}^{\text{mrg}}$ alone. This correction (if it remains small until merger) might therefore further improve the agreement between EOB and NR. However, the current analytical result derived in [41] for $E_{\text{EOB}}^{\text{Schott}}$ is only given in a non-resummed PN form, which cannot be meaningfully applied to the moment of merger. Indeed, when trying to use it to determine its effect on the above NR/EOB comparison, we realized that the PN correction factor was, numerically, of the form $1 - a/c^2 + b/c^4$ with both a/c^2 and b/c^4 positive and of order one at merger (and with $a/c^2 \approx 1 + b/c^4$, suggesting that the whole correction factor is significantly smaller than one). We leave to future work the study of possible *resummations* of the Schott-energy results of [41]. It is only when such (well-tested) resummations are constructed that it will become meaningful to take into account deviations from the naive conservation-laws used above.

IV. FINAL BLACK HOLE STATE

Let us now compare the NR results for the final dynamical state of the system, M_f^{NR} , J_f^{NR} , to the results obtained by subtracting from the EOB predictions for

the dynamical state of the system at merger the subsequent (NR-computed) ringdown losses. In other words, we define, on the EOB side

$$M_f^{\text{EOB[NR]}} := E_{\text{EOB}}^{\text{mrg}} - E_{\text{NR}}^{\text{rgd}}, \quad (24)$$

$$J_f^{\text{EOB[NR]}} := J_{\text{EOB}}^{\text{mrg}} - J_{\text{NR}}^{\text{rgd}}. \quad (25)$$

This comparison is essentially equivalent to the one done in the previous Section, being just the other side of the same coin. However, it is interesting in itself to formulate the NR/EOB comparison in terms of final state quantities (rather than merger ones) both because the final-state parameters are of more physical interest than the merger ones, and because this comparison updates the one made in our previous work [26].

Table IV summarizes the NR/EOB comparison of final (mass-)energy M_f and angular momentum J_f , as well as the corresponding dimensionless Kerr parameter $\hat{a}_f := J_f/M_f^2$. The fractional level of EOB/NR agreement is again (as a consequence of the merger agreement above) at the 10^{-3} level, as shown in Table V. For instance, in the equal-mass case (where the larger number of available multipoles, $\ell_{\text{max}} = 8$, allowed a better determination of the ringdown losses) the absolute agreement between $\hat{a}_{\text{NR}} = 0.68646(4)$ (where the notation (4) indicates the NR probable error on the last digit) and $\hat{a}_{\text{EOB[NR]}} = 0.68590$ is $\hat{a}_{\text{EOB[NR]}} - \hat{a}_{\text{NR}} = -5.6 \times 10^{-4}$.

Up to here we have only considered the NR/EOB comparison for the mass ratios $q = (1, 2, 3, 4, 6)$ simulated with the SpEC code [30, 31]. Such mass ratios are of prime importance for the upcoming ground-based gravitational-wave detectors. However, larger mass ratios can be relevant within more general contexts, such as astrophysical studies of merging BH’s, or future space-based gravitational-wave detectors. One of the advantages of having an accurate analytical understanding of the dynamics of coalescing BHs, such as the one provided by EOB theory, is that one can predict quantities of direct physical interest (such as M_f and \hat{a}_f) for mass ratios that are difficult to simulate with good accuracy. In addition EOB theory provides predictions for the continuous range of ν values, thereby accomplishing both an interpolation and an extrapolation of the information gathered by NR simulations of a discrete sample of q values. Indeed, by inserting now in Eqs. (24),(25) the

TABLE IV. Properties of the final BH: comparison between NR and EOB[NR] predictions.

ν	q	M_f^{NR}	$M_f^{\text{EOB[NR]}}$	J_f^{NR}	$J_f^{\text{EOB[NR]}}$	\hat{a}_f^{NR}	$\hat{a}_f^{\text{EOB[NR]}}$
0.1224...	6	0.98547(5)	0.985754	0.36171(10)	0.361486	0.37245(10)	0.372009
0.16	4	0.97792(2)	0.978440	0.45100(10)	0.450880	0.47160(10)	0.470969
0.1875	3	0.97128(1)	0.971960	0.50997(2)	0.509754	0.54058(2)	0.539590
$0.\bar{2}$	2	0.96124(2)	0.962115	0.57605(4)	0.575565	0.62344(4)	0.621785
0.25	1	0.95162(2)	0.952830	0.62164(4)	0.622704	0.68646(4)	0.685884

TABLE V. Fractional differences between EOB[NR] and NR for the mass, the angular momentum and the dimensionless Kerr parameter of the final BH, defined as $\Delta Q_f/Q_f = (Q_f^{\text{EOB[NR]}} - Q_f^{\text{NR}})/Q_f^{\text{NR}}$ with $Q = M, J$ or \hat{a} .

ν	q	$\Delta M_f/M_f$	$\Delta J_f/J_f$	$\Delta \hat{a}_f/\hat{a}_f$
0.1224...	6	$+2.88 \times 10^{-4}$	-6.06×10^{-4}	-1.18×10^{-3}
0.16	4	$+5.32 \times 10^{-4}$	-2.77×10^{-4}	-1.34×10^{-3}
0.1875	3	$+7.00 \times 10^{-4}$	-4.35×10^{-4}	-1.83×10^{-3}
$0.\bar{2}$	2	$+9.10 \times 10^{-4}$	-8.37×10^{-4}	-2.65×10^{-3}
0.25	1	$+1.27 \times 10^{-3}$	$+1.73 \times 10^{-3}$	-8.20×10^{-4}

polynomial fits (15) of the ringdown losses (instead of the NR-computed losses), we can transform calculations of the dynamical state at merger into estimates of the dynamical quantities M_f , J_f and \hat{a}_f , of the final BH. Before reporting the results of such EOB[NR] calculations for generic values of ν , let us compare what they give in the three specific higher- q cases that have been recently numerically simulated by Lousto and collaborators [32–34]. The results of this comparison are displayed in Table VI. There is a good agreement between the two sets of results. For instance, the absolute (rather than fractional) differences between the values of \hat{a}_f are all of the order of 10^{-4} . It is difficult to put these differences in perspective because Refs. [32–34] do not provide estimates of the probable uncertainty on their (numerically very challenging) results.

In Table VII we give more results of the EOB[NR] predictions for the final masses and spin-parameters of coalescing BH’s, as a function of the symmetric mass ratio ν . Though, by downloading the freely available EOBIHES code [29] [and using Eqs. (15),(24),(25)] any reader can compute such values, it might be useful to encapsulate our results by means of some fitting formulas. Let us first give accurate “local fits” for the ν dependence of M_f and \hat{a}_f interpolating between the Caltech-Cornell-CITA NR results [30, 31]. We found that the following

TABLE VI. Final mass and dimensionless final Kerr parameter: comparison with estimates from Lousto *et al.* [32–34].

ν	q	M_f^{NR}	$M_f^{\text{EOB[NR]}}$	\hat{a}_f^{NR}	$\hat{a}_f^{\text{EOB[NR]}}$
0.0098...	100	0.999382	0.999379	0.0333	0.0334146
0.05859...	15	0.99493	0.994897	0.18875	0.188834
0.08264...	10	0.99174	0.991899	0.2603	0.260176

polynomials

$$\hat{a}_f^{\text{NRfit}}(\nu) = \sqrt{12}\nu + (41.59\nu^3 - 37.3036\nu^2 + 13.9195\nu - 4.6713)\nu^2, \quad (26)$$

$$M_f^{\text{NRfit}}(\nu) = 1 + \left(\sqrt{\frac{8}{9}} - 1\right)\nu + (-2.962\nu^2 + 0.765\nu - 0.5514)\nu^2, \quad (27)$$

reproduce, within their quoted probable errors, the NR results, for the sample of ν values corresponding to the NR q sample $q = (1, 2, 3, 4, 6)$. More precisely, the differences $|\hat{a}_f^{\text{NRfit}}(\nu) - \hat{a}_f^{\text{NR}}(\nu)|$ and $|M_f^{\text{NRfit}}(\nu) - M_f^{\text{NR}}(\nu)|$ are smaller than 1.8×10^{-6} and 6.9×10^{-6} respectively. These fits are more accurate than the ones given in [22, 26, 36, 37], and can therefore be advantageously used in the EOB code to estimate the characteristics of the final BH, when one is interested in q values within the range $1 \leq q \lesssim 6$. [Let us correct in passing a small misprint in Eq. (32) of [24]: its left-hand-side should read a_f/M_f .]

On the other hand, if one is interested in having simple analytical representations of the variation of M_f and \hat{a}_f over the full range $0 < \nu \leq 0.25$, it might be useful to have fits that approximately encapsulate our new EOB[NR] results (a sample of which is displayed in Tables IV, VI, VII, as well as VIII below). For this case, we found that the following “global fits” for the ν depen-

TABLE VII. EOB[NR] predictions for the mass and dimensionless Kerr parameter of the final BH calculated using EOB results at merger together with the fits (15) of the losses.

ν	q	$M_f^{\text{EOB[NR]}}$	$\hat{a}_f^{\text{EOB[NR]}}$
0.02	47.979...	0.998627	0.0672678
0.04	22.956...	0.996862	0.131453
0.06	14.598...	0.994736	0.193092
0.08	10.403...	0.992255	0.252480
0.1	7.8729...	0.989408	0.309825

dence of M_f and \hat{a}_f might be adequate:

$$\hat{a}_f^{\text{EOB[NR]fit}}(\nu) = \sqrt{12}\nu + (255.5\nu^3 - 146.5\nu^2 + 31.467\nu - 5.5534)\nu^2, \quad (28)$$

$$M_f^{\text{EOB[NR]fit}}(\nu) = 1 + \left(\sqrt{\frac{8}{9}} - 1\right)\nu + (-4.815\nu^2 + 1.315\nu - 0.579)\nu^2, \quad (29)$$

Note, however, that the latter fits are less accurate (compared to current NR data) than the former ones, when evaluated at the NR q sample $q = 1, 2, 3, 4, 6$. More precisely, for these values of q the maximum differences $|\hat{a}_f^{\text{NRfit}}(\nu) - \hat{a}_f^{\text{NR}}(\nu)|$ and $|M_f^{\text{NRfit}}(\nu) - M_f^{\text{NR}}(\nu)|$ are only smaller than 1.4×10^{-3} and 3.7×10^{-4} respectively.

Let us finally discuss the extent to which our new EOB[NR] results for M_f and \hat{a}_f represent an improvement with respect to our previous work [26], which used a purely analytical (3PN-accurate) EOB formalism, together with ν^2 -scaled ringdown losses, inferred from an early test-mass calculation [42]. A quantitative comparison of the results of [26] with the present ones is provided in Table VIII. The results of [26] displayed here correspond to the then a priori preferred Damour-Gopakumar-type [25] radiation reaction. As, indeed, this (non-Keplerian) type of resummation of the leading-order term in the waveform (and radiation reaction) plays a crucial role in the resummed EOB radiation reaction [6] incorporated in the current EOB formalism, it is appropriate to contrast them here with the new EOB results. Note, in particular, that, in the $q = 1$ case, the old (3PN-accurate) EOB result of [26] was $\hat{a}_f^{\text{EOB[3PN]}} = 0.7023$. The EOB/NR agreement has been improved by a factor $(0.7023 - 0.68646)/(0.68590 - 0.68646) \simeq -30$. This improvement in the EOB/NR agreement is further illustrated in Fig. 4 which compares the 3PN-accurate earlier predictions of [26] both to the predictions of the current (5PNlog+NR) EOB[NR] predictions, and to the recent NR results. This confirms the trend discussed in [26] (which notably compared 2PN-accurate versions of EOB to 3PN-accurate ones): the addition of more accurate physics in the EOB formalism leads, at the end, to a better agreement with NR results.

TABLE VIII. From left to right the columns report: the symmetric mass ratio ν , the final dimensionless angular momentum \hat{a}_f and the final mass M_f for both the most recent (5PN with logs, NR-completed) EOB formalism of Ref. [24] and the earlier 3PN-accurate (without NR completion) EOB formalism of Ref. [26].

ν	$M_f^{5\text{PNlog+NR}}$	$M_f^{3\text{PN}}$	$\hat{a}_f^{5\text{PNlog+NR}}$	$\hat{a}_f^{3\text{PN}}$
0.01	0.999366	0.9994	0.00340769	0.0341
0.02	0.998627	0.9986	0.0672678	0.0675
0.04	0.996862	0.9969	0.131453	0.1322
0.06	0.994736	0.9949	0.193092	0.1946
0.08	0.992255	0.9925	0.252480	0.2549
0.10	0.989408	0.9898	0.309825	0.3134
0.14	0.982538	0.9834	0.418981	0.4251
0.1825	0.973223	0.9751	0.527487	0.5370
0.2227	0.961923	0.9659	0.622867	0.6373
0.25	0.952830	0.9589	0.685884	0.7023

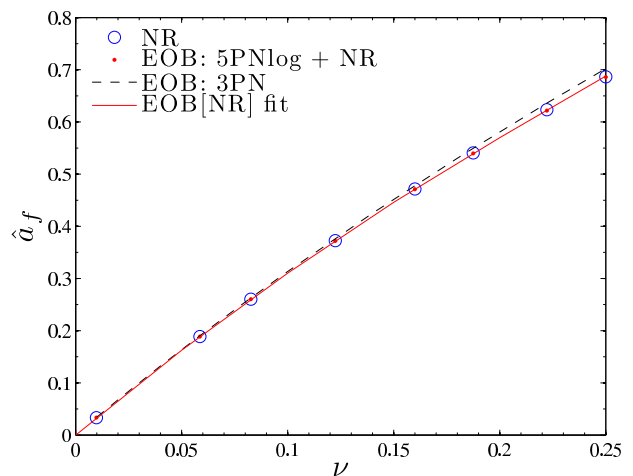


FIG. 4. Dimensionless Kerr parameter as a function of ν : comparison of NR data [30, 31], current (5PNlog+NR) EOB[NR] predictions and their global fit, and earlier (3PN accurate) EOB estimates (joined plot) [26].

V. CONCLUSIONS

The main results of the present investigation are:

- (i) We presented a new quantitative test of the ability of EOB theory to accurately describe the dynamics of coalescing binary BH's. This test goes beyond recent such tests [27, 28] in that it deeply probes the strong-gravitational-field regime. We found that EOB theory predicts values for the energy and angular momentum of the binary system at the moment of merger which agree, to the per mil level, with corresponding values that were inferred from recent accurate NR computations [30, 31]. In a sense, this aspect of our work is an extension of the recent study of the gauge-invariant energy-angular-

momentum relation [28] from the inspiral regime down to the fully relativistic regime of merger.

- (ii) Our work is also an update of a previous EOB study of the final mass and spin of a coalescing binary BH [26]. While the latter study used a purely analytical (3PN-accurate) EOB formalism, completed by ν^2 -scaled test-mass estimates of the ringdown losses, we have used here a recently developed (analytically more complete, NR-informed) EOB formalism [24, 29], together with refined, NR-based estimates of the ringdown losses (based on Refs. [30, 31]). We then find that this leads to a much increased agreement between NR and EOB (e.g. by a factor $\simeq 30$ for the final spin parameter). This confirms the trend found in [26]: the addition of more accurate physics in the EOB formalism leads, at the end, to a better agreement with NR results. In our opinion, this shows that EOB theory, beyond giving a phenomenologically useful description of the gravitational-wave emission of coalescing binaries, does also provide a simple, but physically correct description of the dynamical state of a binary BH system, down to the moment of merger.
- (iii) Another potentially useful outcome of our study concerns the exponential decay with multipolar order ℓ of the integrated losses of energy and angular momentum during ringdown. We showed how this decay can be used to improve the sum over ℓ . Essentially, we proposed a Richardson extrap-

olation of the sum to infinite ℓ_{\max} . We also gave explicit ν -dependent fits of the ratio between the dominant $\ell m = 22$ contribution and the sum of all the subdominant ones. Such fits might be useful for estimating the total losses in cases where NR simulations recorded only the dominant $\ell m = 22$ multipole.

- (iv) From the practical point of view, our work also provides several simple fitting formulas that might be useful in various contexts. For instance, we provide both global and local fits for the mass-ratio dependence of the final mass and spin parameters of (non spinning) coalescing binaries, which incorporate the most recent, accurate NR results (together, in the case of the global fit, with the results of our present EOB[NR] study).

ACKNOWLEDGMENTS

We thank the Caltech-Cornell-CITA collaboration for making available the numerical waveform data of Refs. [30, 31]; we are grateful to Luisa Buchman and Harald Pfeiffer for informative communications about their simulations. We also thank Sebastiano Bernuzzi for his continuous help in improving the EOBIHES code [29] that we used in this work. LV thanks IHES for hospitality during the development of this work.

-
- [1] A. Buonanno and T. Damour, Phys. Rev. D **59**, 084006 (1999)
 - [2] A. Buonanno and T. Damour, Phys. Rev. D **62**, 064015 (2000)
 - [3] T. Damour, P. Jaranowski and G. Schaefer, Phys. Rev. D **62**, 084011 (2000)
 - [4] T. Damour, Phys. Rev. D **64**, 124013 (2001)
 - [5] A. Buonanno, Y. Chen and T. Damour, Phys. Rev. D **74**, 104005 (2006) [gr-qc/0508067].
 - [6] T. Damour, B. R. Iyer and A. Nagar, Phys. Rev. D **79**, 064004 (2009) [arXiv:0811.2069 [gr-qc]].
 - [7] T. Damour, arXiv:1212.3169 [gr-qc].
 - [8] F. Pretorius, Phys. Rev. Lett. **95**, 121101 (2005) [gr-qc/0507014].
 - [9] M. Campanelli, C. O. Lousto, P. Marronetti and Y. Zlochower, Phys. Rev. Lett. **96**, 111101 (2006) [gr-qc/0511048].
 - [10] J. G. Baker, J. Centrella, D. -I. Choi, M. Koppitz and J. van Meter, Phys. Rev. Lett. **96**, 111102 (2006) [gr-qc/0511103].
 - [11] F. Pretorius, arXiv:0710.1338 [gr-qc].
 - [12] H. P. Pfeiffer, Class. Quant. Grav. **29**, 124004 (2012) [arXiv:1203.5166 [gr-qc]].
 - [13] A. H. Mroue, M. A. Scheel, B. Szilagyi, H. P. Pfeiffer, M. Boyle, D. A. Hemberger, L. E. Kidder and G. Lovelace *et al.*, arXiv:1304.6077 [gr-qc].
 - [14] A. Buonanno, G. B. Cook and F. Pretorius, Phys. Rev. D **75**, 124018 (2007) [gr-qc/0610122].
 - [15] Y. Pan, A. Buonanno, J. G. Baker, J. Centrella, B. J. Kelly, S. T. McWilliams, F. Pretorius and J. R. van Meter, Phys. Rev. D **77**, 024014 (2008) [arXiv:0704.1964 [gr-qc]].
 - [16] A. Buonanno, Y. Pan, J. G. Baker, J. Centrella, B. J. Kelly, S. T. McWilliams and J. R. van Meter, Phys. Rev. D **76**, 104049 (2007) [arXiv:0706.3732 [gr-qc]].
 - [17] T. Damour, A. Nagar, E. N. Dorband, D. Pollney and L. Rezzolla, Phys. Rev. D **77**, 084017 (2008) [arXiv:0712.3003 [gr-qc]].
 - [18] T. Damour, A. Nagar, M. Hannam, S. Husa and B. Bruegmann, Phys. Rev. D **78**, 044039 (2008) [arXiv:0803.3162 [gr-qc]].
 - [19] T. Damour and A. Nagar, Phys. Rev. D **79**, 081503 (2009) [arXiv:0902.0136 [gr-qc]].
 - [20] A. Buonanno, Y. Pan, H. P. Pfeiffer, M. A. Scheel, L. T. Buchman and L. E. Kidder, Phys. Rev. D **79**, 124028 (2009) [arXiv:0902.0790 [gr-qc]].
 - [21] Y. Pan, A. Buonanno, L. T. Buchman, T. Chu, L. E. Kidder, H. P. Pfeiffer and M. A. Scheel, Phys. Rev. D **81**, 084041 (2010) [arXiv:0912.3466 [gr-qc]].
 - [22] Y. Pan, A. Buonanno, M. Boyle, L. T. Buchman, L. E. Kidder, H. P. Pfeiffer and M. A. Scheel, Phys. Rev. D **84**, 124052 (2011) [arXiv:1106.1021 [gr-qc]].

- [23] A. Taracchini, Y. Pan, A. Buonanno, E. Barausse, M. Boyle, T. Chu, G. Lovelace and H. P. Pfeiffer *et al.*, Phys. Rev. D **86**, 024011 (2012) [arXiv:1202.0790 [gr-qc]].
- [24] T. Damour, A. Nagar and S. Bernuzzi, Phys. Rev. D **87**, 084035 (2013)
- [25] T. Damour and A. Gopakumar, Phys. Rev. D **73**, 124006 (2006) [gr-qc/0602117].
- [26] T. Damour and A. Nagar, Phys. Rev. D **76**, 044003 (2007) [arXiv:0704.3550 [gr-qc]].
- [27] A. Le Tiec, A. H. Mroue, L. Barack, A. Buonanno, H. P. Pfeiffer, N. Sago and A. Taracchini, Phys. Rev. Lett. **107**, 141101 (2011) [arXiv:1106.3278 [gr-qc]].
- [28] T. Damour, A. Nagar, D. Pollney and C. Reisswig, Phys. Rev. Lett. **108**, 131101 (2012) [arXiv:1110.2938 [gr-qc]].
- [29] The corresponding “EOBIHES” code developed in Ref. [24] and written in **MatLab** is freely available at <http://eob.ihes.fr>.
- [30] M. A. Scheel, M. Boyle, T. Chu, L. E. Kidder, K. D. Matthews and H. P. Pfeiffer, Phys. Rev. D **79**, 024003 (2009) [arXiv:0810.1767 [gr-qc]].
- [31] L. T. Buchman, H. P. Pfeiffer, M. A. Scheel and B. Szilagyi, Phys. Rev. D **86**, 084033 (2012) [arXiv:1206.3015 [gr-qc]].
- [32] C. O. Lousto and Y. Zlochower, Phys. Rev. D **83**, 024003 (2011) [arXiv:1011.0593 [gr-qc]].
- [33] C. O. Lousto, H. Nakano, Y. Zlochower and M. Campanelli, Phys. Rev. D **82**, 104057 (2010) [arXiv:1008.4360 [gr-qc]].
- [34] C. O. Lousto and Y. Zlochower, Phys. Rev. Lett. **106**, 041101 (2011) [arXiv:1009.0292 [gr-qc]].
- [35] S. Bernuzzi, A. Nagar and A. Zenginoglu, Phys. Rev. D **84**, 084026 (2011) [arXiv:1107.5402 [gr-qc]].
- [36] L. Rezzolla, E. Barausse, E. N. Dorband, D. Pollney, C. Reisswig, J. Seiler and S. Husa, Phys. Rev. D **78**, 044002 (2008) [arXiv:0712.3541 [gr-qc]].
- [37] W. Tichy and P. Marronetti, Phys. Rev. D **78**, 081501 (2008) [arXiv:0807.2985 [gr-qc]].
- [38] E. Barausse and L. Rezzolla, Astrophys. J. **704**, L40 (2009) [arXiv:0904.2577 [gr-qc]].
- [39] E. Barausse, V. Morozova and L. Rezzolla, Astrophys. J. **758**, 63 (2012) [arXiv:1206.3803 [gr-qc]].
- [40] C. Reisswig, N. T. Bishop, D. Pollney and B. Szilagyi, Class. Quant. Grav. **27**, 075014 (2010) [arXiv:0912.1285 [gr-qc]].
- [41] D. Bini and T. Damour, Phys. Rev. D **86**, 124012 (2012) [arXiv:1210.2834 [gr-qc]].
- [42] A. Nagar, T. Damour and A. Tartaglia, Class. Quant. Grav. **24**, S109 (2007) [gr-qc/0612096].